Surface Science 651 (2016) 187–194

Contents lists available at ScienceDirect

Surface Science

journal homepage: www.elsevier.com/locate/susc

Complexity of H-bonding between polar molecules on Si(100)-2 × 1 and Ge(100)-2 × 1 surfaces

Xiang Huang [a,b,c], Ren-Yu Tian [a], Xiao-BaoYang [a], Yu-Jun Zhao [a,b,*]

[a] Department of Physics, South China University of Technology, Guangzhou 510640, PR China
[b] Key Laboratory of Advanced Energy Storage Materials of Guangdong Province, South China University of Technology, Guangzhou 510640, PR China
[c] School of Materials Science and Engineering, South China University of Technology, Guangzhou 510640, PR China

ARTICLE INFO

Article history:
Received 24 December 2015
Received in revised form 23 April 2016
Accepted 23 April 2016
Available online 26 April 2016

Keywords:
Hydrogen bond
Si(100)
Ge(100)
Polar molecule
First-principles calculation

ABSTRACT

The adsorption of various combinations of three polar molecules (NH_3, H_2O, and HF) on Si/Ge(100) surface is studied by first-principles calculations. On a given pre-adsorbed substrate, the H-bonding and dative bonding always show a synergistic effect, together with the electrostatic attraction, dominating the adsorption and dissociation of polar molecules on Si/Ge(100). Both H_2O and HF are found to be energetically favored to cluster with the pre-adsorbed H_2O molecule on Si/Ge(100) surface. Catalyzed by H_2O, the dissociation barriers of H_2O on Ge(100) decrease from ~0.7 to ~0.4 eV, in comparison with the nearly an order of magnitude reduction on Si(100). Furthermore, H_2O molecule dissociates spontaneously on Si(100) and the barriers are lowered to ~0.2 eV on Ge(100) when catalyzed by HF, providing an efficient approach for dissociation of H_2O on Si(100) and Ge(100) surfaces.

1. Introduction

The modification of Si/Ge(100) surface with various compounds has become a topic of interest in the past decades, since it provides a basis for emerging fields such as microelectronic, biological recognition, and chemical sensors [1,2]. Previous researches mainly focused on surface reactivity [2–11]. It is well known, however, that the vast majority of molecules possess dipoles, such as HF (1.91 D), H_2O (1.85 D), CH_3OH (1.70 D), and NH_3 (1.47 D) [12]. When they interact with Si/Ge(100)-2 × 1 surface, the dipole interactions between molecules themselves such as H-bonding, and between molecule and the surface, including electrostatic interaction and dative bonding will become complicated [13–15].

Generally, H-bonding is considered as a weak interaction among polar molecules, such as H_2O, NH_3, and HF. Nevertheless, it seems to be a ubiquitous phenomenon that, once a polar molecule has dative-bonded with Si(100) surface, the H-bonding between which and the additional molecule from the gas phase would be remarkably strengthened. For example, the H-bond of a H_2O dimer on Si(100) is shortened significantly from 1.88 Å (a free H_2O dimer) to 1.36 Å; and as a result the dissociation barriers are lowered by a magnitude compared to a single H_2O molecule [16]. The phenomena are similar to that of NH_3 on Si(100), where the H-bond is shortened from 2.24 (a free NH_3 dimer) to 1.74 Å, and the dissociation barriers are lowered as half as that of a single NH_3 [17]. In particular, the H_2O molecules are energetically favored to cluster via H-bonding on Si(100) [16]. That is to say, H-bonding has played an important role in the adsorption and dissociation of polar molecules on Si(100) surface, which helps explain the dissociation of H_2O/NH_3 on Si(100) at low temperatures [18–22]. However, the mechanism therein is not well understood yet. On the other hand, we note that similar phenomenon also exists on Ge(100), where H_2O molecules are partially dissociated at low temperature (~100 K) [23,24]. We are expecting to gain more insight into the mechanism, through choosing different polar molecules to interact with Si(100) and Ge(100) surfaces.

Herein, we first investigate the adsorption of isolated HF, H_2O, and NH_3 molecules on Si(100) and Ge(100) substrates, respectively. The adsorption of H_2O and NH_3 is found to be dative bonding dominated, while HF is classical electrostatic attraction dominated. Then we investigate the adsorption of different combinations of these three polar molecules on H_2O or NH_3 pre-adsorbed Si(100) and Ge(100) substrates. It is found that H-bonding shows a synergistic effect with the dative bonding, together with electrostatic attraction, dominating the adsorption and dissociation of the polar molecules on Si/Ge(100). In particular, both H_2O and HF molecules from the gas phase are energetically favored to cluster with the pre-adsorbed H_2O on Si(100) and Ge(100). Catalyzed by H_2O, the dissociation barriers of H_2O on Ge(100) are remarkably reduced compared to the isolated H_2O, leading to an explanation of

* Corresponding author at: Department of Physics, South China University of Technology, Guangzhou 510640, PR China.
E-mail address: zhaoyj@scut.edu.cn (Y.-J. Zhao).

http://dx.doi.org/10.1016/j.susc.2016.04.010
0039-6028/

the dissociation of H_2O on Ge(100) at low temperatures. Catalyzed by HF, H_2O molecule dissociates spontaneously on Si(100) and the barriers are lowered to ~0.2 eV on Ge(100).

2. Computational framework

All the calculations are carried out based on the density functional theory (DFT) as implemented in Vienna ab initio simulation package (VASP) with consideration of spin-polarization [25]. The exchange and correlation potential is approximated by the generalized gradient approximation with the PBE functional [26], which has been proved to present a good evaluation on the adsorption energy for molecule adsorption on Si(100) surface [27]. Electronic wave functions are expanded using a plane-wave basis set with a cutoff energy of 400 eV. Dispersion correction, which takes van der Waals (vdW) interaction into consideration, is considered through DFT-D2 method as proposed by Grimme [28]. Our discussions are mainly based on the data with dispersion correction since it is regarded to have a better description of the adsorption structures and corresponding energies than those of standard DFT [29].

The Ge(100) and Si(100) surfaces are simulated by a periodic slab model of $Ge_{48}H_{16}$ and $Si_{48}H_{16}$ with a $c(2 \times 4)$ periodicity in a supercell throughout the simulations, respectively. The slab is composed of six atomic layers with the bottom layer passivated by 16 H atoms, and the vacuum spacing is about 11 Å. To check the possible artificial electric field effect caused by an asymmetric slab, the total energies of a H_2O molecule in X-pointed configuration on Ge(100) and Si(100) surfaces are calculated with thicker vacuum layers, respectively. The difference in total energies of slabs from ~11 Å to ~20 Å is within 8 meV for Ge(100), and nearly unchanged for Si(100). The Brillouin-zone is sampled using Monkhorst-Pack mesh of $4 \times 2 \times 1$ k points for the calculations, and the difference in adsorption energy of a H_2O in X-pointed configuration is within 4 meV on Ge(100) and nearly unchanged on Si(100) when the mesh increases to $6 \times 3 \times 1$. The calculated bond lengths for the Ge–Ge and Si–Si dimers are 2.59 and 2.36 Å respectively, in good agreement with earlier theoretical [30,31] and experimental data [32,33]. All the coordinates are fully relaxed until the residual force (Hellmann–Feynman forces) on each atom is within 0.02 eV/Å, except the two fixed bottom Ge/Si layers and the passivating H layer. The minimum energy pathways (MEPS) for the dissociation are determined using the climbing image nudged elastic band (CI-NEB) method [34]. Considering computational costs, five or seven images are simultaneously optimized along reaction pathway until the force in each image is smaller than 0.05 eV/Å. The saddle point configuration is further refined by minimizing the forces until 0.02 eV/Å value is reached. We have further conducted a test CI-NEB calculation with 10 images for the OD and ID procedures of H_2O dimer on Ge(100) surface. It is found that the reaction barriers change within 5 meV with respect to that from 5 images. In addition, we have evaluated the zero-point energy (ZPE) from both initial and transition states on reaction barrier [35].

3. Adsorption of polar molecules on Si/Ge(100) surface

Three typical polar molecules, H_2O, NH_3, and HF, have been chosen to interact with Si(100) and Ge(100) surfaces, which appear as rows of buckled dimers. As charges deplete at the down-atom of the dimer, a dative bonding is likely to form following Lewis acid–base interaction, where the charge is transferred from the lone pair of electrons of X atom (X = O, N and F) to the down-atom. Of note, there exists intrinsic intermolecular H-bonding among H_2O, NH_3, and HF molecules due to their large dipole moments. It provides a possible approach to gain more insight into the phenomenon of H-bonding enhancement through adsorbing various combinations of these polar molecules on Si(100) and Ge(100) substrates.

3.1. Adsorption of an isolated molecule

Before the investigation of different combinations of these polar molecules on Si/Ge(100) surface, it is necessary to figure out the difference among these single molecules when interacted with Si/Ge(100). Two possible configurations of each molecule have been considered: (i) X atom positioned above down-atom of a dimer pair on substrate (X-pointed); and (ii) H atom positioned above up-atom (H-pointed), according to the electrostatic attraction. The adsorption energy (E_{ads}) is obtained through subtracting the sum of total energies of clean substrate and isolated molecule from that of X-pointed or H-pointed configuration, as listed in Table 1.

The stability of two types of configurations shows an opposite trend on both substrates. For H-pointed configuration, the order of E_{ads} is HF > H_2O > NH_3, while the order is HF < H_2O < NH_3 for X-pointed configuration. It is known that a stronger electronegativity corresponds to a weaker ability of donating lone pair of electrons. That is, for a specific acceptor, such as Si_{down} atom, the strength of dative bonding is F…Si < O…Si < N…Si, which can be concluded from the dative bond length: F…Si > O…Si > N…Si in spite of the atomic radii follow N > O > F (cf. Fig. 1).

On the other hand, a stronger electronegativity also means that the H atom of X—H bond loses more charge. As a result, the classical electrostatic attraction between H atom and up-atom becomes stronger, which is in line with the trend of distance between H and Si_{up} atom: F—H…Si < O—H…Si < N—H…Si, as shown in Fig. 1.

For H_2O and NH_3, the X-pointed configurations are significantly more stable than those at H-pointed. For example, E_{ads} of NH_3 are 1.26 and 0.86 eV on Si(100) and Ge(100), while those at H-pointed configurations are only 0.06 and 0.05 eV. It indicates that dative bonding has dominated the adsorption of H_2O and NH_3. However, for HF we find that the stability of two configurations is comparable. Given that $E_{ads}$of H-pointed configuration is almost derived from the classical electrostatic attraction, it indicates that electrostatic attraction has played a dominant role in the adsorption of HF.

3.2. Adsorption of additional molecule

Considering the significant E_{ads} of X-pointed configurations of H_2O and NH_3 on Si(100) and Ge(100) substrates, $Si(100)^{H2O}$, $Ge(100)^{H2O}$, $Si(100)^{NH3}$, and $Ge(100)^{NH3}$ surfaces are chosen as the pre-adsorbed substrates, on which three polar molecules are further to adsorb. Here, $Si(100)^{H2O}$ represents the H_2O adsorbed Si(100) surface, and others follow this rule. The adsorption configurations are shown in Fig. 2, with corresponding parameters listed in Table 2. The adsorption energy (E_{ads}) of the additional molecule is defined as:

$$E_{ads} = -[E_{M/pre\text{-}adsorbed\text{-}F(100)} - E_{pre\text{-}adsorbed\text{-}F(100)} - E_M],$$

Where $E_{M/pre\text{-}adsorbed\text{-}F(100)}$, $E_{pre\text{-}adsorbed\text{-}F(100)}$, and E_M represent the total energies of pre-adsorbed substrate with the additional adsorbed molecule, pre-adsorbed substrate, and isolated molecule, respectively. F denotes Ge/Si element. M denotes molecule (H_2O, NH_3, and HF).

Table 1
The adsorption energies of isolated HF, H_2O, and NH_3 molecules on Si(100) and Ge(100) surfaces with H- and X-pointed configurations, respectively. The experimental data of dipole moments for these molecules are also listed. Values in parenthesis are the corresponding results with van der Waals correction.

		E_{ads}/Si(100) (eV)		E_{ads}/Ge(100) (eV)	
Molecule	Dipole moment	X-pointed	H-pointed	X-pointed	H-pointed
HF	1.91	0.29(0.40)	0.29(0.34)	0.24(0.39)	0.24(0.31)
H_2O	1.85	0.71(0.87)	0.13(0.18)	0.43(0.62)	0.10(0.16)
NH_3	1.47	1.26(1.46)	0.06(0.12)	0.86(1.09)	0.05(0.13)

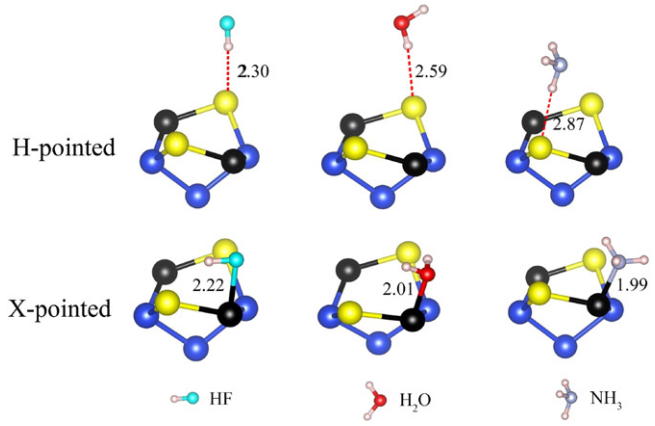

Fig. 1. X-pointed and H-pointed configurations of HF, H_2O, and NH_3 on Si(100) surface. Black and yellow balls represent Si_{down} and Si_{up} atoms, respectively. Of note, the molecules have similar H- and X-pointed configurations on Ge(100) surface.

3.2.1. Various combinations of polar molecules on Si/Ge(100) surface

Overall, we find that E_{ads} of the additional molecule is contributed from synergistic effect and electrostatic attraction.

A. Synergistic effect.
From all of the optimized configurations, we observe that the X—H bond engaged in H-bonding is elongated to some extent, and the dative bond is shortened. It is due to a strong H-bonding of X'…H—X weakening the covalent X—H bond, and naturally the dative bonding of X…Ge/Si is enhanced. That is to say, a great H-bonding always accompanies with a large dative bonding, thus showing a synergistic effect, as shown schematically in Fig. 3a. Therefore, it is reasonable to adopt the elongation ratio (χ) of X—H bond to characterize the strength of H-bonding. Here we define: $\chi = \frac{l'-l}{l}$, in which l and l' represent the length of X—H bond of pre-adsorbed molecule before and after H-bonding. Correspondingly, the contraction ratio (η) of X…Ge/Si bond is used to describe the strength of dative bonding. It is defined as:$\eta = \frac{L-L'}{L}$, where L and L' represent the length of X…Ge/Si bond before and after H-bonding.

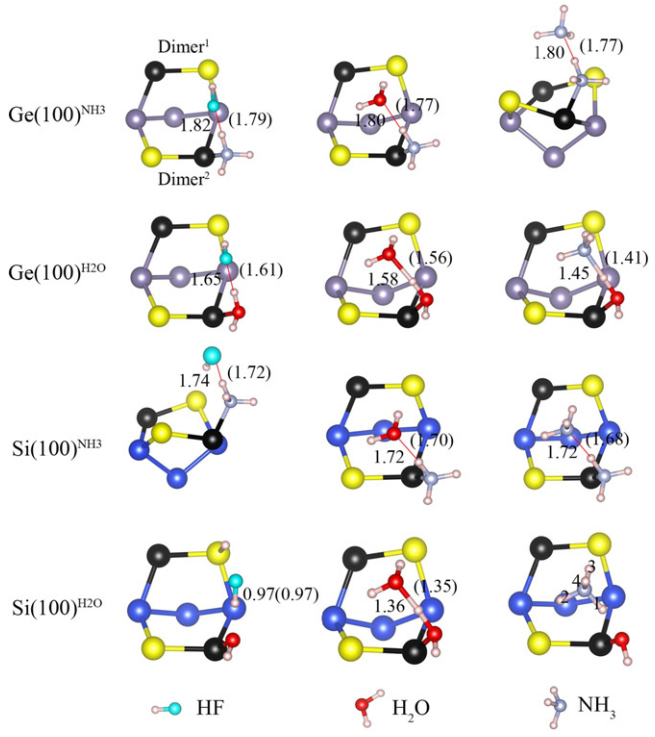

Fig. 2. Adsorption of HF, H_2O, and NH_3 on $Ge(100)^{NH3}$, $Ge(100)^{H2O}$, $Si(100)^{NH3}$, and $Si(100)^{H2O}$ surfaces, respectively. Values in brackets are revised by vdW correction. Black and yellow balls represent corresponding down and up atoms, respectively. The lengths of N-H_1 to N-H_4 are in the range of 1.03–1.08 Å, indicating the formation of $[NH_4]^{\delta+}$ ($0 < \delta < 1$) group. The length of H—F is 0.97 Å on $Si(100)^{H2O}$ surface, closing to 0.94 Å of its free state, indicating that a new HF molecule has been formed.

Generally, the synergistic effect is influenced by the electronegativity of X atom of the additional molecule, dative bonding, as well as the polarity of X—H bond of pre-adsorbed molecule.

i. Electronegativity of X atom of the additional molecule
On a specific pre-adsorbed substrate (except $Si(100)H_2O$), it is found that $\chi$and η always show an increasing trend with the adsorption from HF, H_2O, to NH_3, seen in Fig. 3b. It indicates that the synergistic effect is enhanced in this sequence. Note that the components that engaged in H-bonding is mostly localized at X' atom and X—H bond, as shown in Fig. 3a, the difference in χ is mainly ascribed to the electronegativity of X atom. That is to say, the strength of H-bonding is analogous to that of dative bonding: the weaker electronegativity of X atom is, the stronger H-bonding will be, i.e., NH3 > H2O > HF.

ii. Dative bonding
For the same additional molecule, the H-bonds on Si(100)NH3 surface are found to be 0.07–0.10 Å shorter than that on Ge(100)NH3 surface, seen in Fig.2. Similar difference also exists between Ge(100)H2O and Si(100)H2O. For instance, H-bond of H_2O dimer on Si(100) is 1.35 Å, 0.21 Å shorter than that on Ge(100). To gain a deeper understanding, we replaced the occupied Ge atom on Ge(100) by a Si atom (the substrate is denoted as Sub I), and re-optimized H_2O dimer configuration on it. The projected density of states (PDOS) shows that, the energy levels of the dative bonded O, H, and the H-bonded O atoms on Sub I are shifted toward lower energies with respect to that on Ge(100) surface (cf. Fig. 4a and b). In particular, the hybridized level appeared at −10.27 eV on Ge(100) shifts to −10.98 eV on Sub I. The calculated local partial density of states in the energy range of −11.2 to −10.8 eV confirms that it is an H-bond interaction. The charge density difference between Sub I and Ge(100) showed a remarkable charge accumulation in the region between two H_2O molecules, seen in Fig.4c. It means that the H-bond has transformed to a covalence bond to some extent on Sub I, indicating that H-bond is further enhanced on Si(100) as compared to that on Ge(100). This is attributed to a superior dative bonding of Si…O to Ge…O, which improves the polarity of OH bond, and thereby enhances the intermolecular H-bonding.

iii. Polarity of X—H bond of pre-adsorbed molecule
Though the Ge…O dative bonding is not as strong as Ge…N, for the same additional molecule the length of H-bond on $Ge(100)H_2O$ is found to be remarkably shorter than that on Ge(100)NH3, as shown in Fig 2. For example, the H-bond of NH_3 on $Ge(100)NH_3$ is 1.77 Å, while it is shortened to 1.41 Å when replaced the pre-adsorbed NH3 to H_2O, which possesses a much larger dipole moment. Correspondingly, E_{ads} is increased by 0.26 eV. It indicates that the dipole moment of X—H bond of pre-adsorbed molecule is also a crucial factor for H-bonding. Here the dipole moment of O—H bond of H_2O is about 0.2 D larger than that of N—H bond of NH_3.

B. Electrostatic attraction
Throughout all these configurations, we find that the X—H bonds of the additional molecules are always inclined to point to the up-atoms on the substrate. That means the electrostatic interaction between the molecule and substrate also contributes to the adsorption energy, in addition to synergistic effect.
Especially, on a specific pre-adsorbed substrate (except $Si(100)^{H2O}$), we find that the corresponding χ or η is always showing an

Table 2
The adsorption energies (E_{ads}) of the additional molecule on $Ge(100)^{NH3}$, $Ge(100)^{H2O}$, $Si(100)^{NH3}$, and $Si(100)^{H2O}$ surfaces. Pre-NH_3 and Pre-H_2O denote the pre-adsorbed NH_3 and H_2O on Si(100) and Ge(100) substrates. X—Ge/Si, X—H, Dimer, Δh(Dimer) are representative of the lengths of X—Ge/Si dative bond, X—H bond engaged in H-bonding of the pre-adsorbed molecule, dimer, and vertical height between two dimer atoms, respectively. χ and η denote the elongation ratio of X—H bond and contraction ratio of X—Ge/Si bond, respectively. X represents O, N or F atom. The vdW corrected lengths of X—H and X—Ge/Si bonds (shown in parenthesis) are used to calculated χ and η.

	E_{ads} (eV)	X—H (Å)	χ(%)	X—Ge(Si) (Å)	η(%)	$Dimer^1$(Å)	$Dimer^2$(Å)	Δh($Dimer^1$)(Å)	Δh($Dimer^2$)(Å)
Ge(100)	–	–	–	–	–	2.59	2.59	0.88	0.88
Pre-NH_3	–	1.03(1.03)	–	2.19(2.18)	–	2.62	2.57	0.70	0.85
HF	0.58(0.69)	1.04(1.04)	0.97	2.15(2.14)	1.8	2.63	2.55	0.65	0.77
H_2O	0.51(0.68)	1.05(1.05)	1.9	2.13(2.12)	2.8	2.62	2.55	0.65	0.83
NH_3	0.55(0.72)	1.07(1.07)	3.9	2.12(2.11)	3.2	2.63	2.56	0.64	0.84
Pre-H_2O	–	0.98(0.99)	–	2.30(2.29)	–	2.61	2.57	0.75	0.85
HF	0.62(0.73)	1.01(1.01)	2.0	2.18(2.16)	5.7	2.62	2.55	0.69	0.77
H_2O	0.64(0.80)	1.03(1.03)	4.0	2.14(2.13)	7.0	2.62	2.56	0.68	0.84
NH_3	0.79(0.98)	1.11(1.14)	15	2.08(2.06)	10	2.63	2.56	0.65	0.84
Si(100)	–	–	–	–	–	2.36	2.36	0.77	0.77
Pre-NH_3	–	1.03(1.03)	–	1.99(1.98)	–	2.42	2.35	0.52	0.74
HF	0.71(0.80)	1.05(1.05)	1.9	1.96(1.95)	1.5	2.43	2.36	0.45	0.69
H_2O	0.62(0.77)	1.06(1.07)	3.7	1.94(1.94)	2.0	2.43	2.35	0.47	0.74
NH_3	0.64(0.81)	1.09(1.10)	6.4	1.93(1.92)	3.0	2.43	2.35	0.44	0.73
Pre-H_2O	–	1.00(1.00)	–	2.01(2.00)	–	2.40	2.36	0.55	0.75
HF	1.85(1.96)	–	–	1.72(1.71)	–	2.45	2.39	0.24	0.42
H_2O	0.87(1.01)	1.12(1.12)	12	1.86(1.85)	7.5	2.43	2.35	0.47	0.75
NH_3	1.30(1.49)	–	–	1.75(1.75)	–	2.46	2.35	0.37	0.71

increasing trend from HF, H_2O, to NH_3, shown in Fig. 3b. It suggests that the contribution of synergistic effect to E_{ads} is in the order of $NH_3 > H_2O >$ HF. To one's surprise, only E_{ads} of NH_3 and H_2O follow the trend, while HF does not. For example, E_{ads} of HF is found to be slightly greater than that of H_2O on $Ge(100)^{NH3}$ or $Si(100)^{NH3}$, seen in Fig. 3c.

Given that E_{ads} resulted from synergistic effect and electrostatic attraction, we speculate that the contribution from the classical electrostatic attraction is remarkable in HF case. We find that the vertical height of $Dimer^2$ of Si/Ge(100) varies most before and after the additional adsorption. For example, the vertical height of $Dimer^2$ on Ge $(100)^{NH3}$ is decreased by 0.08 Å after HF adsorption, while only 0.02 Å and 0.01 Å for H_2O and NH_3 adsorption, respectively (cf. Table 2). The similar trends also exist on $Ge(100)^{H2O}$ and $Si(100)^{NH3}$. It indicates that the classical electrostatic attraction between HF and substrate is much more remarkable than that of H_2O and NH_3, in line with the adsorption of isolated molecule on Ge(100) and Si(100).

3.2.2. Spontaneous dissociation of pre-adsorbed H_2O on Si(100)

On $Si(100)^{H2O}$, for the adsorption of HF and NH_3, the pre-adsorbed H_2O molecule dissociates spontaneously in the process of optimization, along with formation of a new HF molecule and $[NH_4]^{\delta+}$ ($0 < \delta < 1$) group, as shown in Fig. 2. The pre-adsorbed H_2O molecule on Si(100), however, does not dissociate when H-bonded with the additional H_2O. Given that the synergistic effect follows the trend of $NH_3 > H_2O >$ HF on a specific pre-adsorbed substrate, it indicates that the formation of a new HF molecule is mainly attributed to the remarkable electrostatic attraction of HF with substrate. The formation of $[NH_4]^{\delta+}$ is likely ascribed to the greater synergistic effect between NH_3 and pre-adsorbed H_2O.

Furthermore, it can be speculated that with the formation of more H-bonds, the synergistic effect will be further enhanced. Herein, we have investigated the adsorption of a H_2O/NH_3 tetramer on Si(100). It is found that the pre-adsorbed H_2O/NH_3 dissociates spontaneously, as shown in Fig. 5, indicating that synergistic effect is greatly strengthened compared to the case of H_2O/NH_3 dimer.

4. Dissociation of H_2O on Ge(100) surface at low temperature

4.1. Clustering of H_2O molecules on Ge(100) surface

Similar to the cases on Si(100), the enhancement of H-bonding also exists on Ge(100). Particularly, the adsorption energy of H_2O on $Ge(100)^{H2O}$ via H-bonding is about 0.64 eV, 0.21 eV larger than that of X-pointed configuration. It implies that clustering of H_2O is likely an energetically favored process on Ge(100).

Based on X-pointed configuration of H_2O on Ge(100), we consider the possible configuration of the additional H_2O molecule's adsorption, which can be classified into two scenarios. One is directly adsorbed on Ge atoms near the occupied Ge_{down}, the other is adsorbed around the pre-adsorbed H_2O via H-bonding, as shown in Fig. 6.

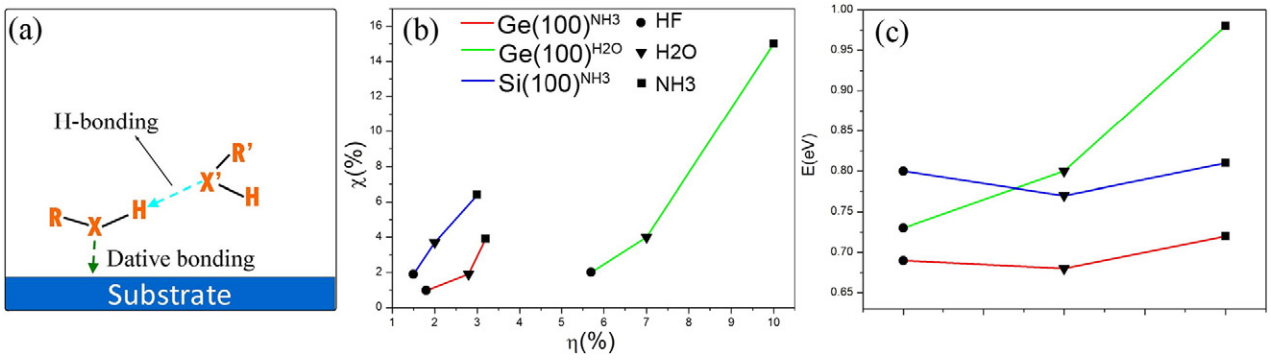

Fig. 3. (a) Schematic of an additional molecule (R'-X'H) H-bonding with the pre-adsorbed molecule (R-XH) on Si/Ge(100) substrate. X and X' denote F, O, and N atoms, and R and R' represent the other components in the molecule. (b) Elongation ratio (χ) of X—H bond versus contraction ratio (η) of X—Ge/Si for the additional adsorption of HF, H_2O, and NH_3 on $Ge(100)^{NH3}$, $Ge(100)^{H2O}$, and $Si(100)^{NH3}$, respectively. (c)$E_{ads}$of HF, H_2O, and NH_3 on these three pre-adsorbed substrates.

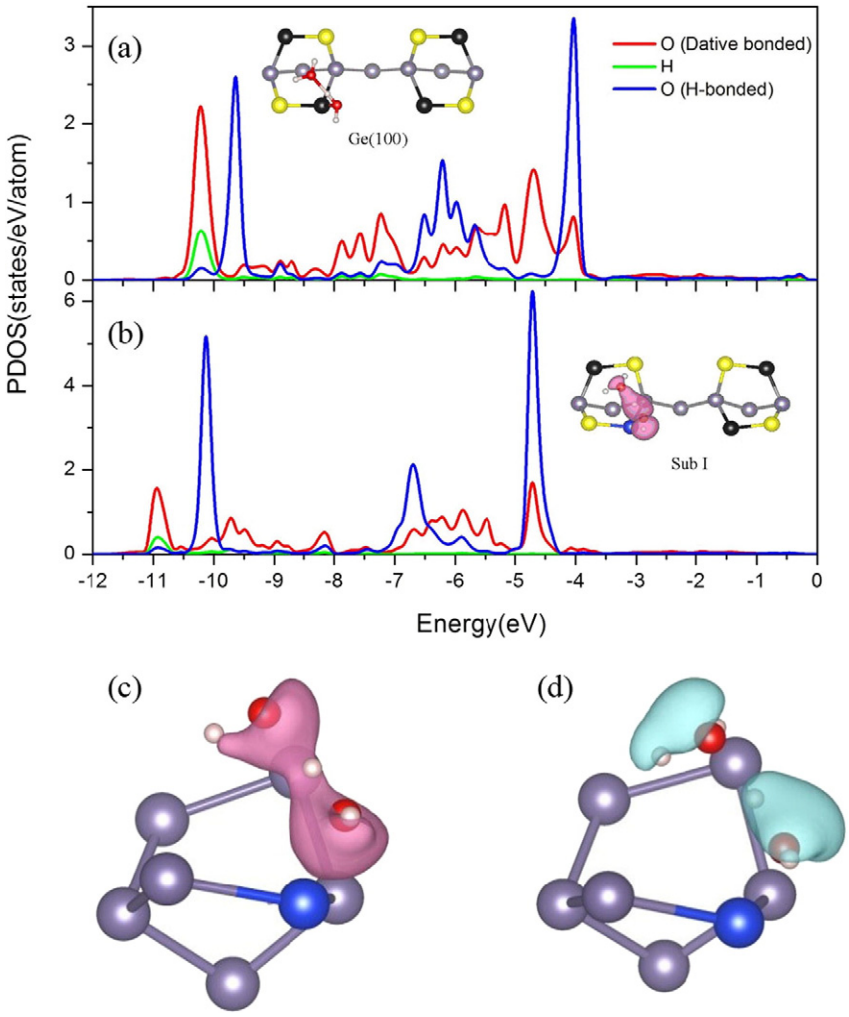

Fig. 4. (a)–(b) Projected density of states (PDOS) for the dative bonded O, H, and the H-bonded O atoms of configuration of H_2O dimer on Ge(100) and Sub I, respectively. The energy levels are aligned with respect to the 1*s* level of the Ge atom in the bulk layer. The Fermi level of configuration of H_2O dimer on Sub I is set to zero. Inset of (b) is the local partial density of states calculated in the energy range of −11.2 to −10.8 eV. (c)–(d) Isosurface plots of charge density difference [$\rho(Si_{down})$-$\rho(Ge_{down})$]. Here, purple/light blue represents electron accumulation/depletion. $\rho(Ge_{down})$ and $\rho(Si_{down})$ denote total charge density of configuration of H_2O dimer on Ge(100) and Sub I, respectively. The gray and blue balls denote Ge atoms and Si atom, respectively. The isosurface levels are ±0.015 electrons/bohr^3.

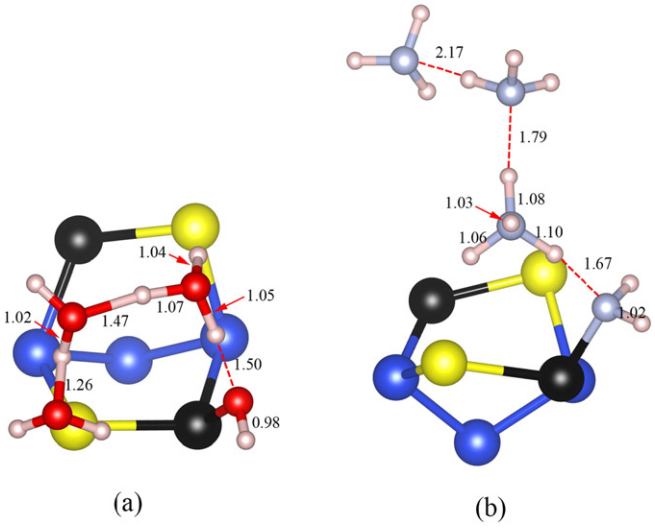

Fig. 5. Adsorption configuration of H_2O (a) and NH_3 (b) tetramers on Si(100) surface. The bond lengths are in the unit of Å.

The adsorption energy (E_{ads}) of the additional H_2O molecule is defined as:

$$E_{ads} = -[E_{Ge(100)^{2H2O}} - E_{Ge(100)^{H2O}} - E_{H_2O}],$$

Where $E_{Ge(100)^{2H2O}}$, $E_{Ge(100)^{H2O}}$, and E_{H_2O} are representative of the total energies of $Ge(100)^{2H2O}$, $Ge(100)^{H2O}$, and isolated H_2O molecule, respectively. Overall, configurations f, g, and h are energetically comparable, with the relatively larger adsorption energies of 0.76, 0.80, and 0.80 eV after vdW correction, respectively. Together with configuration e, it is found that all the clustered configurations (configurations e-h) are more stable with respect to the configurations adsorbed directly on substrate (cf. Table 3). That is to say, the H_2O molecule in the gas phase is energetically favored to H-bond with pre-adsorbed one, rather than adsorb dispersedly on the substrate. The initial configurations of the second H_2O at I, III, and IV sites are H_2O floating above the dimer with O atom pointed to the Ge_{up} atoms. Nevertheless, after optimization the H_2O molecules at sites I and III transform to H-bond with the pre-adsorbed H_2O, as shown in Fig. 6e and 6f, respectively. The H_2O molecule at site IV changes the orientation with H pointed to Ge_{up} atom (cf. Fig. 6d), with adsorption energy of 0.18 eV. Despite a similar initial location of H_2O on Ge(100) and Si(100) substrates, the optimized configurations of H_2O at III, and IV sites are different from those on

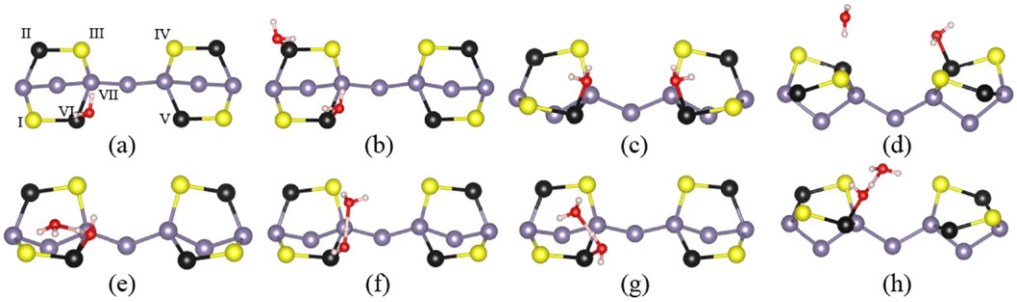

Fig 6. Configurations of the additional H_2O adsorbed on Ge(100). (a) Sketch map of the possible adsorption sites for the second H_2O molecule on $Ge(100)^{H2O}$ surface. The optimized configurations for H_2O adsorbed on Ge atoms near the occupied Ge_{down} (b–d) and around the pre-adsorbed H_2O via H-bonding (e–h). The yellow and black balls represent Ge_{up} and Ge_{down} atoms in the first layer, respectively. The gray balls denote the Ge atoms in the second and third layers.

Si(100), where the Si_{up} in III and IV sites change into Si_{down} and dative bond with H_2O eventually. On the one hand, it is attributed to the electrostatic interaction between the H atom of H_2O and the Ge_{up} atom. On the other hand, the calculated flipping barrier of Ge–Ge dimer is 0.41 eV, larger than that of Si–Si dimer (0.26 eV). As for configurations b and c, the adsorption energies of the second H_2O is 0.57 and 0.61 eV, both smaller than that of pre-adsorbed H_2O, implying that there exists classical electrostatic repulsion between the adjacent H_2O molecules. However, the barriers for breaking the dative bonding of configurations b and c and diffusing to H-bond with the pre-adsorbed H_2O, corresponding to configurations g and h, are only 0.21 and 0.12 eV, respectively, as shown in Fig. 7a and 7b. Therefore, even if H_2O molecules have adsorbed dispersedly at Ge_{down} atoms, they will be easily clustered due to the small diffusion barriers.

4.2. Dissociation of H_2O on Ge(100)

We first consider the dissociation barriers of an isolated H_2O on Ge(100). Since the dissociated H atom of H_2O is likely to bond with Ge_{up} atom at the same dimer or inter-dimer, as shown in Fig.8, we name these two dissociation pathways as OD and ID procedures. The calculated barriers are 0.77 and 0.71 eV for OD and ID procedures, respectively, both larger than the molecular adsorption energy of H_2O. It suggests that the adsorbed H_2O molecule on Ge(100) prefers to desorb before dissociation, in line with the dramatically small sticking probability of H_2O on Ge(100) at room temperature [23,36].

However, for the dissociation of a H_2O dimer, driven by a greater synergistic effect, the donor H atom is gradually moved away from the pre-adsorbed H_2O to the additional one. When reaching the saddle point, the original H-bond between H_2O molecules is shortened to 1.05–1.08 Å, close to the OH bond of H_2O molecule at free state (0.97 Å), while the OH bond of the pre-adsorbed H_2O molecules is elongated to 1.43–1.50 Å, gradually displaying H-bond character. Simultaneously, the OH bond of the additional H_2O pointed to the Ge_{up} atom is elongated to 1.32–1.36 Å, due to the electrostatic attraction between H and Ge_{up} atoms. Finally, the pre-adsorbed H_2O dissociates and a new H_2O molecule forms on the substrate. The local structures of transition states of the possible OD and ID procedures for configurations e–h are shown in Fig.7c.

Compared to an isolated H_2O, the barrier is lowered from 0.77 to 0.45 eV for the OD procedure, and from 0.71 to 0.40 eV for the ID procedure. In particular, the barriers are further lowed by 0.1–0.2 eV by the vdW and ZPE corrections, as listed in Table 4. It well explains the experiment observation that H_2O molecules could dissociate at low temperature (~100 K) [23,24]. Throughout all of these reaction pathways, it is found that ID procedures have lower barriers than those of OD procedures (cf. Table 4). Particularly, the barrier for configuration f is only 0.19 eV. Thus we speculate that the ID products probably exist on Ge(100) surface, though only OD products have been observed so far as the reported experiments are limited [37].

On Si(100), the pre-adsorbed H_2O dissociates spontaneously under the catalysis of HF [38]. It is dominated by the remarkable electrostatic attraction between HF and Si(100) substrate as compared to H_2O and NH_3. Hereafter we consider several configurations of HF on $Ge(100)^{H2O}$. Two stable configurations are shown in Fig. 8, corresponding to OD and ID procedures. Their adsorption energies are 0.58 and 0.62 eV, respectively, both greater than 0.24 eV of the X-pointed configuration on Ge(100). It indicates that HF is energetically favored to H-bond with pre-adsorbed H_2O on Ge(100). Subsequently, we calculate the dissociation barriers of OD and ID procedures, which are 0.22 and 0.21 eV, both prevailing over the H_2O molecule itself. Considering that the synergistic effect of H_2O dimer on Ge(100) is greater than that between HF and pre-adsorbed H_2O, it indicates that electrostatic attraction of HF with Ge(100) has played a dominant effect on the dissociation. Significantly, it provides a better way to facilitate the dissociation of H_2O on Si(100) and Ge(100) surfaces.

Table 3
Relative adsorption energy (E_{ads}) of the second H_2O in configurations b–h on the pre-adsorbed Ge(100)-$c(2\times4)$ before and after vdW correction.

	a	b	c	d	e	f	g	h
E_{ads} (eV)	0.43	0.37	0.41	0.12	0.61	0.65	0.64	0.67
E_{ads}-vdW (eV)	0.62	0.57	0.61	0.18	0.71	0.76	0.80	0.80

5. Conclusion

We have investigated the adsorption of isolated HF, H_2O, and NH_3, and their various combinations on Si(100) and Ge(100) substrates. It is found that both the isolated H_2O and NH_3 tend to dative bond with the substrates, while the electrostatic attraction has played a dominant role for the adsorption of HF. On a given pre-adsorbed substrate, H-bonding shows a synergistic effect with the dative bonding, together with electrostatic attraction, dominating the adsorption and dissociation of polar molecules on Si/Ge(100).

In particular, H_2O and HF molecules from the gas phase are found to be energetically favored to cluster with the pre-adsorbed H_2O on Si(100) and Ge(100). Driven by the synergistic effect, the dissociation barriers of H_2O on Ge(100) are reduced from ~0.7 to ~0.4 eV as compared to the isolated H_2O. It well explains the experimental phenomena that H_2O molecules could dissociate at low temperature.

Additionally, HF is found to be an excellent catalyst for H_2O dissociation due to a large electrostatic attraction with Si/Ge(100) surface. Catalyzed by HF, H_2O dissociates spontaneously on Si(100) and the barriers are lowered to ~0.2 eV on Ge(100). This provides an effective approach for dissociation of H_2O on Si(100) and Ge(100) surfaces.

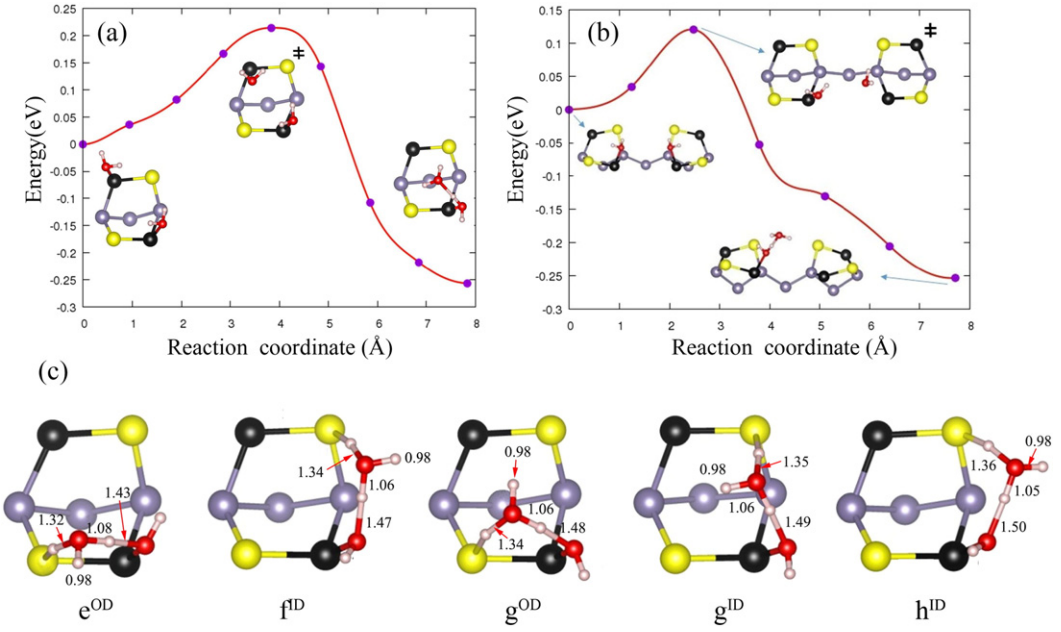

Fig. 7. (a)–(b) Two diffusion pathways corresponding to transformations from configuration b to g, and from configuration c to h, respectively. The insets correspond to the initial state, transition state, and final state, respectively. (c) Local structures of transition states of the possible OD and ID procedures for configurations e–h.

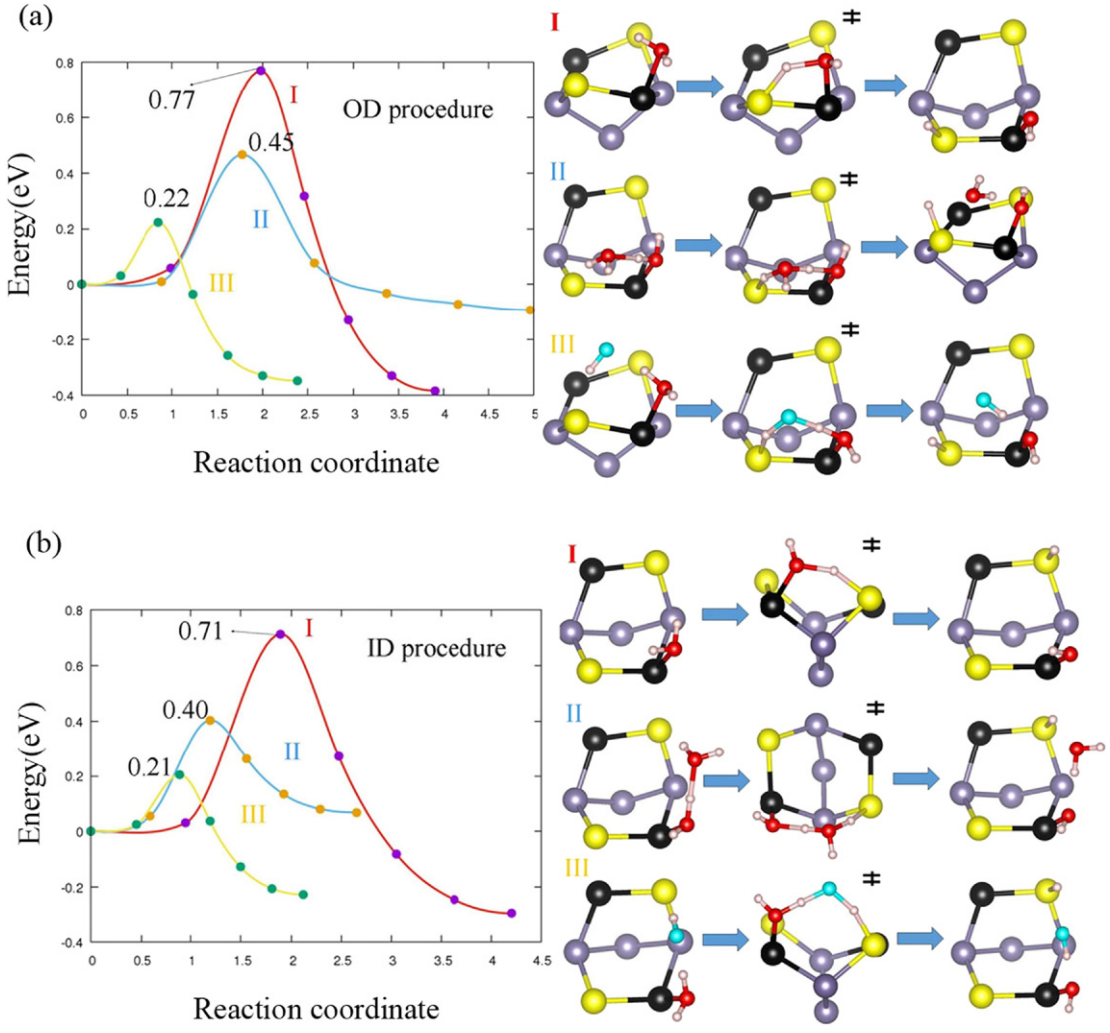

Fig. 8. The potential energy curves and dissociative pathways (initial, transition, and final states) of OD and ID procedures for (I) an isolated H_2O, (II) H_2O–H_2O cluster and (III) H_2O-HF cluster are shown in (a) and (b), respectively.

Table 4
Calculated dissociation barriers of procedures OD and ID for the pre-adsorbed H_2O, and configurations e–h. Values in parenthesis are corresponding to data with vdW correction and vdW + ZPE (zero point energy) corrections, respectively. No dissociation path is available for the cases without calculated barrier data.

Barrier (eV)	a	e	f	g	h
OD procedure	0.77 (0.77, 0.61)	0.45 (0.42, 0.25)	–	0.56 (0.56, 0.35)	–
ID procedure	0.71 (0.68, 0.51)	–	0.40 (0.38, 0.19)	0.49 (0.48, 0.29)	0.45 (0.43, 0.30)

Acknowledgments

This work is supported by NSFC (grant 11574088, 51431001), the Fundamental Research Funds for the Central Universities (grant 2015ZP010, 2015PT017), and KLGHEI (KLB11003). The computer times at National Supercomputing Center in Guangzhou (NSCCGZ) are gratefully acknowledged.

Appendix A. Supplementary data

Supplementary data to this article can be found online at http://dx.doi.org/10.1016/j.susc.2016.04.010.

References

[1] S.F. Bent, Surf. Sci. 500 (2002) 879.
[2] M.A. Filler, S.F. Bent, Prog. Surf. Sci. 73 (2003) 1.
[3] T.R. Leftwich, A.V. Teplyakov, Surf. Sci. Rep. 63 (2008) 1.
[4] T.B. Lim, I.R. McNab, J.C. Polanyi, H. Guo, W. Ji, J. Am. Chem. Soc. 133 (2011) 11534.
[5] K.R. Harikumar, T. Lim, I.R. McNab, J.C. Polanyi, L. Zotti, S. Ayissi, W.A. Hofer, Nat. Nanotechnol. 3 (2008) 222.
[6] T. Lim, J.C. Polanyi, H. Guo, W. Ji, Nat. Chem. 3 (2011) 85.
[7] M. Satta, R. Flammini, A. Goldoni, A. Baraldi, S. Lizzit, R. Larciprete, Phys. Rev. Lett. 109 (2012) 036102.
[8] S.-Y. Yu, H. Kim, J.-Y. Koo, Phys. Rev. Lett. 100 (2008) 036107.
[9] M. Dürr, U. Höfer, Surf. Sci. Rep. 61 (2006) 465.
[10] I. Lyubinetsky, Z. Dohnálek, W.J. Choyke, J.T. Yates, Phys. Rev. B: Condens. Matter Mater. Phys. 58 (1998) 7950.
[11] D.R. Belcher, M.W. Radny, S.R. Schofield, P.V. Smith, O. Warschkow, J. Am. Chem. Soc. 134 (2012) 15312.
[12] R.D. Nelson Jr., D.R. Lide Jr., A.A. Maryott, Selected Values of Electric Dipole Moments for Molecules in the Gas Phase, in(DTIC Document) 1967.
[13] L. Zhang, Q. Song, S.B. Zhang, Phys. Rev. Lett. 104 (2010) 116101.
[14] K. Yong-Sung, K. Ja-Yong, K. Hanchul, J. Phys. Condens. Matter 21 (2009) 064237.
[15] Y.-S. Kim, J.-Y. Koo, H. Kim, Phys. Rev. Lett. 100 (2008) 256105.
[16] X. Huang, R.-Y. Tian, X.-B. Yang, Y.-J. Zhao, J. Phys. Chem. C 118 (2014) 24603.
[17] M. Satta, R. Flammini, A. Goldoni, A. Baraldi, S. Lizzit, R. Larciprete, Phys. Rev. Lett. 109 (2012) 036102.
[18] W. Ranke, Surf. Sci. 369 (1996) 137.
[19] Y.J. Chabal, S.B. Christman, Phys. Rev. B: Condens. Matter Mater. Phys. 29 (1984) 6974.
[20] F. Bozso, P. Avouris, Phys. Rev. Lett. 57 (1986) 1185.
[21] J.L. Bischoff, F. Lutz, D. Bolmont, L. Kubler, Surf. Sci. 248 (1991) L240.
[22] I.R. Challis, J.W. Adcock, Surf. Sci. 304 (1994) 33.
[23] L. Papagno, D. Frankel, Y. Chen, L.S. Caputi, J. Anderson, G.J. Lapeyre, Surf. Sci. 248 (1991) 343.
[24] T.-F. Teng, W.-L. Lee, Y.-F. Chang, J.-C. Jiang, J.-H. Wang, W.-H. Hung, J. Phys. Chem. C 114 (2010) 1019.
[25] G. Kresse, J. Furthmüller, Phys. Rev. B: Condens. Matter Mater. Phys. 54 (1996) 11169.
[26] J.P. Perdew, M. Ernzerhof, K. Burke, J. Chem. Phys. 105 (1996) 9982.
[27] H.-J. Kim, A. Tkatchenko, J.-H. Cho, M. Scheffler, Phys. Rev. B: Condens. Matter Mater. Phys. 85 (2012) 041403.
[28] S. Grimme, J. Comput. Chem. 27 (2006) 1787.
[29] Z.-X. Hu, H. Lan, W. Ji, Sci. Report. 4 (2014) 5036.
[30] M.W. Radny, G.A. Shah, S.R. Schofield, P.V. Smith, N.J. Curson, Phys. Rev. Lett. 100 (2008) 246807.
[31] S.C. Jung, M.H. Kang, Phys. Rev. B: Condens. Matter Mater. Phys. 80 (2009) 235312.
[32] R. Rossmann, H.L. Meyerheim, V. Jahns, J. Wever, W. Moritz, D. Wolf, D. Dornisch, H. Schulz, Surf. Sci. 279 (1992) 199.
[33] S. Ferrer, X. Torrelles, V.H. Etgens, H.A. van der Vegt, P. Fajardo, Phys. Rev. Lett. 75 (1995) 1771.
[34] G. Henkelman, B.P. Uberuaga, H. Jónsson, J. Chem. Phys. 113 (2000) 9901.
[35] D. Sholl, J.A. Steckel, Density Functional Theory: A Practical Introduction, John Wiley & Sons, Inc., Hoboken, New Jersey, 2011.
[36] H.J. Kuhr, W. Ranke, Surf. Sci. 189–190 (1987) 420.
[37] J.Y. Jung, S. Lee, S. Hong, J. Kim, Phys. Chem. B 109 (2005) 24445.
[38] The clustered H_2O and HF dissociate spantaneously on Si(100) with a total energy of final configuration about 1.6 eV lower than that of H_2O and HF adsorbed dispersedly on Si(100). It is reasonable to say that HF is energetically favorable to cluster with the pre-adsorbed H_2O on Si(100).